Ismail Karacan

Department of Textile Engineering,
Faculty of Engineering, Erciyes University,
TR-38039 Kayseri, Turkey
E-mail: ismailkaracan@erciyes.edu.tr

Structure-property Relationships in High-strength High-modulus Polyethyelene Fibres

Abstract
Six commercially available high-strength, high-modulus polyethylene fibres have been studied with the aim of developing a deeper understanding of their structure-property relationships. Structural studies have been carried out on the measurement of crystallite size and orientation parameters using a wide range of techniques including optical microscopy, thermal analysis and wide-angle X-ray diffraction techniques, together with polarised IR spectroscopy. Birefringence, melting temperatures, melting enthalpies and crystallinity values are found to increase with increasing tensile strength and modulus as a direct result of the increased chain alignment induced during the fibre-drawing stages. Careful examination of the results show that improving the chain alignment encourages the alignment and lateral perfection of unoriented non-crystalline chains. Analysis of wide-angle X-ray diffraction, polarised IR spectroscopy and thermal analysis confirms the presence of a three-phase structure consisting of polymorphic crystalline (i.e. orthorhombic and monoclinic), highly oriented non-crystalline (i.e. paracrystalline) and unoriented non-crystalline (i.e. amorphous) structures, as opposed to the classical two-phase (crystalline and amorphous) structures. Analysis of polarised IR data shows the existence of a polymorphic structure consisting of highly oriented orthorhombic and monoclinic crystallites, together with highly oriented non-crystalline structure containing pseudo-hexagonally packed chains. Analysis of second order orientation parameter, $<P_{200}>$, shows that the monoclinic crystallites are more oriented than the orthorhombic crystallites. The analysis of the X-ray diffraction data suggests that increasing crystallinity and lateral perfection leads to a consistent reduction in the proportion of the oriented non-crystalline structure. A scanning electron microscopy (SEM) examination of the longitudinal views showed fibrillar striations along the fibre axis direction, together with relatively smooth surfaces with increasing tensile moduli. The samples showed excellent bending behaviour advantageous for the formation of fabrics. The cross-sectional images appeared to vary from deformed triangular to deformed circular shapes.

Key words: *polyethylen, orientation, crystallinity, infrared spectroscopy, thermal analysis, birefringence, X-ray diffraction.*

Introduction

High-performance fibres of organic and inorganic origin (e.g. carbon, ceramics, glass, etc.) have received serious attention during the last few decades due to their desirable properties such as their high strength, high modulus, high chemical resistance and high thermal stability at elevated temperatures.

The most successful organic-origin high-performance fibres prepared from wholly aromatic rigid moities are based on liquid crystalline polymers originating from lyotropic and/or thermotropic systems. For example, aramids based on poly(p-phenylene terepthalamide) have been introduced on both sides of the Atlantic by DuPont under the trade name of Kevlar® in USA and by Akzo Nobel under the trade name of Twaron® in Europe. Thermotropic polyester based on HBA/HNA copolymer has been introduced by Celanase under the trade name of Vectran®. At the University of Leeds, during the 1980s and early 1990s, considerable research work was carried out on the synthesis [1,2], characterisation [3] and molecular modelling [4-6] of thermotropic polyesters containing rigid chain structures which exhibited liquid crystalline behaviour in the melt.

There have also been similar efforts in improving the mechanical performance of linear flexible-chain polymers such as polyethylene by super-drawing [7-8], solid-state extrusion [9] and gel-spinning techniques [10-11]. In effect, fibres produced from the linear flexible chain polymers by conventional spinning still contain a large proportion of folded chains. By choosing appropriate molecular weight distribution and by drawing at a suitable temperature and rate, folded chains can be partially unravelled to give chain-extended materials at very high draw ratios. Polyethylene fibres with a modulus of around 70 GPa have been produced by the superdrawing technique.

In fact, in practical terms, the most significant progress towards the enhancement of the mechanical properties of PE fibres has been achieved with the development of the process of gel-spinning (i.e. solution spinning followed by drawing at very high draw ratios). This process was discovered, developed and patented in Holland by Dutch State Mines (DSM) and produced under licence in USA by Allied Signal Corp (now Honeywell International Inc). The Dutch products have been introduced under the trade name of Dyneema® whereas the USA products have been introduced under the trade name of Spectra® [12]. These commercially important PE fibres are finding applications in the areas of thermosetting resins, elastomers, ballistic protection and marine applications such as ropes and high performance sailcloths. The gel-spun filaments of polyethylene are reported to be drawn to very high draw ratios leading to a very highly extended structure along the fibre axis direction. Values of tensile strength up to 5 GPa and of Young modulus of 120 GPa have been reported [10-11] for polyethylene filaments made in this way.

In the present investigation, six commercially available gel-spun polyethylene fibres have been studied with the aim of establishing the structure-property relationships in terms of the degree of crystallinity, crystallite size and the states

of the orientation of the crystalline and non-crystalline chains, with the ultimate aim of gaining an improved understanding of the processing-structure-property relationships.

Experimental

Materials

The samples used in the present study were three grades of gel-spun PE fibres commercially produced by Dutch State Mines (DSM) of Holland and Allied Signal (now Honeywell International Inc.) of USA. In total, 6 samples with molecular weights greater than 10^6 daltons were studied in the present study. Details of the samples showing the linear density, density, and mechanical properties are listed in Table 1, where the samples have been identified by their commercial name. Unfortunately, the processing conditions were not made available to us for commercial reasons.

Refractive index measurements

The refractive indices of the fibre samples with the aim of determining birefringence values were measured using an image-splitting Carl Zeiss-Jena interphako interference microscope. The refractive indices in the fibre axis direction ($n_{//}$) and transverse direction ($n_{\perp}$) were measured by matching the refractive index of Cargille immersion liquids. The birefringence of a fibre sample can be defined as the difference between the refractive index for light polarised parallel to the fibre axis, $n_{//}$, and that for light polarised perpendicular to the fibre axis, $n_{\perp}$. The values measured of the refractive indices and the birefringences are shown in Table 2.

Infrared measurements

A Nicolet Magna IR 750 Fourier Transform spectrophotometer, equipped with a ZnSe based wire grid polariser, was employed for infrared dichroic measurements. The polariser remained in a fixed orientation (either vertical or horizontal) throughout the experiments, and the samples were rotated in order to obtain spectra for different polarisation directions.

The directly measured absorbance values were subject to errors due to the imperfect polariser effects. These errors can be corrected according to a procedure developed by Green & Bower [13]. No such corrections were found to be necessary following the previous studies carried out on one-way and two-way drawn polypropylene [14] & PVC films [15], and polyacrylonitrile (PAN)-based acrylic fibres [16] due to the absorbance values being below the critical value of 1.5. In all cases, 200 interferograms of a sample were averaged and transformed by the Happ-Genzel apodisation function. All the spectra were collected at a resolution of 2 cm^{-1}. Finally, all the spectra were analysed by curve fitting procedures to obtain the peak parameters.

DSC measurements

The differential scanning calorimetry (DSC) experiments were carried out using a DuPont Differential Scanning

Table 1. *Sample details; (* Manufacturer's data).*

Sample	Linear density, tex	Density*, g/cm^3	Tensile* strength, GPa	Elongation* at break, %	Young's* modulus, GPa
SPECTRA® 900	1.1988	0.97	2.61	3.6	79
SPECTRA®1000	0.3996	0.97	3.25	2.9	113
SPECTRA®2000	0.3886	0.97	3.25	2.9	116
DYNEEMA®SK60	0.1150	0.97	2.70	3.5	89
DYNEEMA®SK65	0.1130	0.97	3.00	3.6	95
DYNEEMA® SK75	0.2256	0.97	3.40	3.8	107

Table 2. *Refractive index results; (* Ref. 20).*

Sample	$n_{//}$*	$n_{\perp}$*	Δn*	$<P_{200}>_{opt}$
SPECTRA® 900	1.5900	1.5310	0.0590	0.922
SPECTRA® 1000	1.5910	1.5320	0.0590	0.922
SPECTRA® 2000	1.5920	1.5320	0.0600	0.938
DYNEEMA® SK60	1.5900	1.5320	0.0580	0.906
DYNEEMA® SK65	1.5900	1.5320	0.0580	0.906
DYNEEMA® SK75	1.5920	1.5320	0.0600	0.938

Table 3. *Thermal analysis results.*

Sample	T_m, °C	$\%Xc_1$ lamellar crystals	$\%Xc_2$ orthorhombic crystals	$\%Xc_3$ hexagonal mesophase	$\%Xc_4$ monoclinic crystals	%Xc total	ΔH^{20}, J/g
SPECTRA® 900	146	11.1	25.8	32.8	6.1	76	222.2
SPECTRA® 1000	150	10.6	46.5	19.4	-	77	224.3
SPECTRA® 2000	150	4.5	53.4	19.2	-	77	225.9
DYNEEMA® SK60	147	7.7	37.8	25.5	1.0	72	211.1
DYNEEMA® SK65	149	6.9	58.8	11.3	5.6	83	243.4
DYNEEMA® SK75	149	2.0	64.4	9.6	7.1	83	242.0

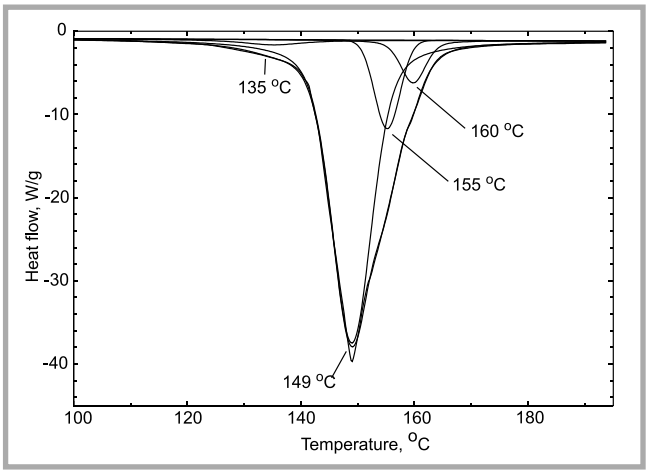

Figure 1. *A typical resolved DSC thermogram of gel-spun polyethylene fibre; (Dyneema® SK65 grade fibre.*

Table 4. X-ray analysis results.

Sample	HKL indexing	Experimental half-height width 2θ, deg	Corrected half-height width 2θ, deg	Integral breadth 2θ, deg	$L_{(hkl)}$ crystallite size due to Stokes, nm	$L_{(hkl)}$ crystallite size due to integral breadth, nm
SPECTRA® 900	110	0.76	0.69	0.86	12.98	10.49
	200	0.78	0.71	0.91	12.66	9.88
SPECTRA® 1000	110	0.69	0.62	0.77	14.48	11.61
	200	0.93	0.86	1.10	10.47	8.21
SPECTRA® 2000	110	0.72	0.66	0.80	13.55	11.29
	200	1.10	1.05	1.22	8.61	7.39
DYNEEMA® SK60	110	1.46	1.40	1.77	6.45	5.10
	200	1.61	1.55	1.95	5.84	4.63
DYNEEMA® SK65	110	1.22	1.16	1.45	7.76	6.20
	200	1.23	1.17	1.41	7.72	6.42
DYNEEMA® SK75	110	1.11	1.04	1.32	8.65	6.81
	200	1.06	1.00	1.20	9.00	7.55

Calorimeter controlled by a Thermal Analyst 2000 system. The typical sample weights used were approximately 5 mg. The heating rate of 20°C/min and an upper temperature range of 200°C were selected. Indium (m.p. 156.5°C) was used as the calibration standard. The specimens were always tested in a nitrogen environment. The results of the DSC measurments carried out are presented in Table 3, whereas a typical resolved DSC thermogram of gel-spun polyethylene fibres is shown in Figure 1.

X-ray diffraction

The wide-angle X-ray traces were obtained using a Scintag X-ray diffractometer system utilising nickel-filtered CuK radiation (at a wavelength of 0.1542 nm) and voltage and current settings of 50 kV and 40 mA respectively. Counting was carried out at 20 steps per degree. The equatorial X-ray scattering data observed in the 10-35° 2θ range was corrected for Lorentz, polarisation and incoherent scatter effects, and finally normalised to a convenient standard area. Intensity-corrected and normalised X-ray data was analysed by the peak fitting procedure detailed earlier [17], assuming a combination of Lorentzian and Gaussing line profiles.

The peak widths at half-height were corrected using Stoke's deconvolution procedure [18]. Finally, the crystallite size of a given reflection was calculated using the Scherrer equation. The resulting crystallite sizes evaluated for the strongly diffracting (110) and (200) reflections using corrected half-height widths of Stoke's deconvolution procedure [18] and the integral-breadths of all polyethylene fibre samples are listed in Table 4.

Scanning Electron Microscopy

The lateral and cross-sectional surface structure of gel-spun polyethylene fibres were examined using an ISI-100A scanning electron microscope with a voltage setting of 5 kV and a specimen detector for distances ranging between 8 mm to 12 mm respectively.

Data analysis

Infrared data - curve fitting

In the present work, the perpendicular and parallel polarisation spectra were fitted according to the procedure described previously [20]. During the IR data collection, an average of 10 experiments for each sample were carried out to maintain the reproducibility of the results.

Infrared data - evaluation of orientation averages

For uniaxially oriented systems with cylindrical symmetry, such as fibres, the calculation of orientation parameters derived from the analysis of the infrared data can be carried out using the dichroic ratio defined by equation (1),

$$D = A_{//} / A_{\perp} \qquad (1)$$

where $A_{//}$ and $A_{\perp}$ are the measured absorbance values for radiation polarised parallel and perpendicular to the fibre axis respectively. To a good approximation, the dichroic ratio is related to the orientation parameter $\langle P_2(\cos\theta)\rangle$ by

$$\langle P_{200}\rangle = \langle P_2(\cos\theta)\rangle = \frac{D-1}{D+2}\cdot\frac{D_o+2}{D_o-1} \qquad 2)$$

where θ is the angle between the chain axis and the fibre axis, and $D_o = 2\cos^2\alpha$, α being the angle between the transition moment associated with the vibrational mode and the chain axis. For samples with very low birefringence, such as the present polyethylene fibre samples, however, equations (1) and (2) are sufficiently accurate. The $\langle P_{200}\rangle$ values may vary between 0.0 and 1. For random orientation, $\langle P_{200}\rangle$ may take the value of 0.0, while for complete orientation the value of $\langle P_{200}\rangle$ is 1.

Evaluation of orientation averages from birefringence values

The second-order orientation parameter, known as Herman's orientation parameter, is determined using equation (3).

$$\langle P_{200}\rangle_{opt} = \frac{\Delta n}{\Delta n^o} \qquad (3)$$

where Δn is defined as the birefringence.

In the present study, a value of 0.064 (corresponding to the measurement of light wavelength of 589.3 nm) has been used as the maximum birefringence (Δn^o) value for the fully oriented sample of polyethylene [21]. The values of Herman's orientation parameter $\langle P_{200}\rangle$ determined from the refractive index data are presented in Table 2.

Evaluation of DSC crystallinity from melting enthalpy values

The degree of DSC crystallinity can be evaluated from the melting enthalpies using Equation (4)

$$X_c = \frac{\Delta H_m}{\Delta H_m^o} \times 100\% \qquad (4)$$

where X_c is the degree of crystallinity evaluated by the DSC method, ΔH_m is the melting enthalpy of the sample, and ΔH_m^o is the melting enthalpy of 100% crystalline sample, and is taken as 293 J/g as published in the literature [20]. DSC crystallinity values are listed in Table 3.

Results and discussion

Optical microscopy data

The birefringence and the refractive index values measured at 589.3 nm are listed in Table 2. The measured birefringence (Δn) values and evaluated $\langle P_{200}\rangle_{opt}$ values show that the polyethylene fibre samples possess very high de-

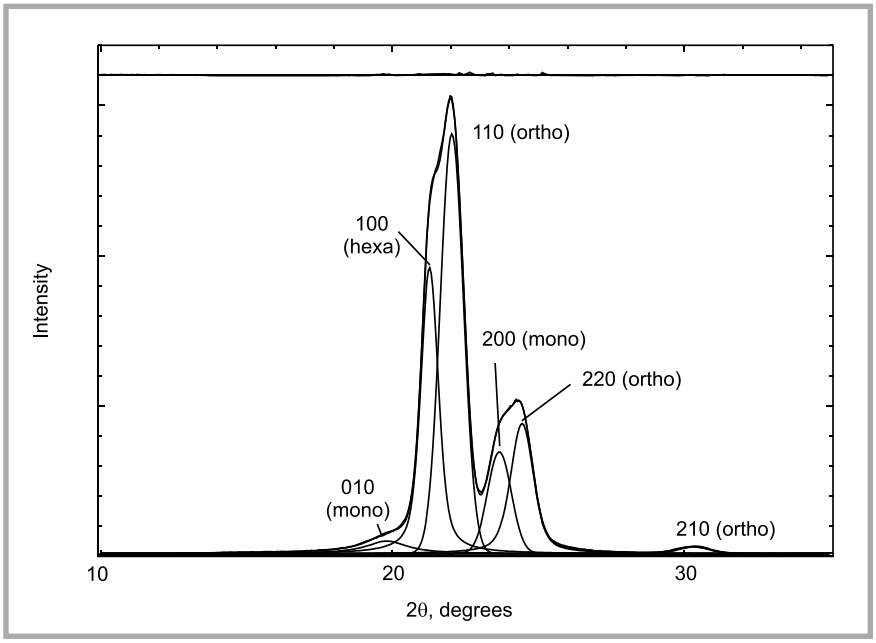

Figure 3. *A typical equatorial wide-angle X-ray diffraction trace (10°-35° 2θ) of gel-spun polyethylene fibre (Dyneema® SK75 grade). The indexing of the reflections are indicated on the figure for the sake of clarification. The lower curves are the fitted peaks; the middle curve is the observed spectrum, and the upper curve is the difference between the observed spectrum and the fitted spectrum on the same scale.*

grees of chain alignment along the fibre axis direction. The average chain angle between the molecular chains and the fibre axis, $\langle\theta_{c,f}\rangle$opt, is found to vary between 11.7 and 14.5°. It should be noted that for perfect molecular orientation, the average orientation angle should be equal or close to 0°. The results suggest that the Spectra® 2000 and Dyneema® SK75 grade PE fibre samples have almost perfect overall orientation, as shown by their high $\langle P_{200}\rangle$opt values listed in Table 2.

Thermal analysis data

Qualitative analysis of DSC traces suggests an asymmetrical melting endotherm between 120 and 175°C with a main peak located around 149-150°C. For a detailed quantitative characterisation of DSC traces, a well-established curve-fitting procedure[17] is applied. As shown in Figure 1, at least 4 melting endotherms can be resolved. The first, weak endotherm located in the 135ºC region is usually assigned to the melting of the folded lamellar crystals. The second, strong endotherm located in the 149ºC region is usually assigned to the melting of the orthorhombic crystals. The shoulder-shaped third endotherm located in the 155ºC region is usually assigned to the melting of the pseudo-hexagonal mesophase. The fourth, weak endotherm located in the 160ºC region is commonly assigned to the melting of the monoclinic structure [21-23].

During the analysis of the curve-fitted DSC traces, it was assumed that the total melting enthalpy between 120 and 175ºC is due to the sum of the melting of the polycrystalline structure consisting of orthorhombic and monoclinic phases, together with the pseudo-hexagonal structure. In the analysis, it has been further assumed that the un-oriented non-crystalline phase known as the amorphous phase makes no contribution to the total melting enthalpy.

The results listed in Table 3 show an increase in the DSC crystallinity ($\%X_c$), calculated as the sum of the proportion of the folded lamellar crystals, orthorhombic and monoclinic crystals (i.e. $\%X_{c1} + \%X_{c2} + \%X_{c4}$ in Table 3) in parallel to the increase in molecular orientation and Young's modulus listed in Tables 1 and 2. It should be noted that folded-chain conformations are incorporated in the lamellar crystals, whereas extended-chain conformations are incorporated in the orthorhombic crystals.

The DSC crystallinity values listed in Table 3 suggests that the PE fibres of US origin contain a fraction of crystalline structure varying between 76-77%, whereas the PE fibres of European origin contain crystalline structure varying between 72-83%. In turn, these crystallinity values suggest amorphous fractions ($1-X_c$) varying between 23-24% for the fibres of US origin and 17-28% for those of European origin.

The results show that the increases in tensile strength and modulus appear to be associated with the increase in the chain alignment (see Tables 1 and 2). As shown in Figure 2, there is also a similar relationship between the tensile modulus and the melting temperature. In effect, the increase in melting temperature is found to be associated with the increasing alignment of chains, which in turn is associated with an improvement in the tensile strength and modulus.

The thermal analysis results presented in Table 3 show that the proportion of folded lamellar crystals decreases with the increase in melting temperatures and enthalpies as a direct consequence of the unravelling processes taking place during the fibre formation stages. This behaviour is in agreement with the increase in overall molecular orientation and Young's modulus values listed in Tables 1 and 2.

Wide-angle X-ray diffraction data

Analysis of equatorial traces from the samples show well-defined peaks. With the aim of obtaining detailed quantitative information, the equatorial traces in the 10-35° 2θ region, shown in Figure 3, can be resolved into 6 peaks indexed as (010 and 200 monoclinic), (100 hexagonal), (110, 200 and 210 orthorhombic) reflections, respectively.

By definition, the area under the baseline is considered to be caused by the amorphous phase. The fraction of the amorphous phase, following the curve fitting procedure, is found to vary between 2 and 3% for the Spectra® grade PE fibres and between 5% and 7% for the Dyneema® grade PE fibres respectively. This in turn suggests that the X-ray crystallinity values vary between 97 and 98% for the PE fibres of US origin and between 93 and 95% for those of European origin. It should be remembered that the X-ray crystallinity values consist of the fractions of polycrystalline phase consisting of orthorhombic and monoclinic crystallites with an oriented pseudo-hexagonal phase respectively.

If we assume that the X-ray diffraction method is a more reliable means of assessing fractional crystallinity and amorphous fraction values, then the amorphous

fraction obtained from thermal analysis appears to overestimate the amorphous fraction. This is due to the assumption that the calculation of DSC crystallinity assumes a two-phase structure consisting of only the presence of crystalline and amorphous phases respectively. In the present investigation, however, the X-ray diffraction method has been able to detect the presence of three-phase structures known as crystalline, oriented non-crystalline (i.e. oriented pseudo-hexagonal) and un-oriented non-crystalline (i.e. amorphous) phases respectively.

The crystallite sizes which are perpendicular to the strongly diffracting (110) and (200) planes of the orthorhombic structure, asevaluated from corrected half-height widths following Stoke's deconvolution procedure, are listed in Table 4. The crystallite size which is perpendicular to the (110) planes of the USA-made Spectra® grade PE fibres varies between 12.98 and 14.48 nm, corresponding to up to 35 chains in this direction. Using the same approach, the European-made Dyneema® grade PE fibres appear to contain up to 21 chains in the same direction. It shows that the USA-made PE fibres contain larger laterally packed orthorhombic structures than the European PE fibres, as shown by the higher number of chains in the direction perpendicular to the (110) diffracting planes.

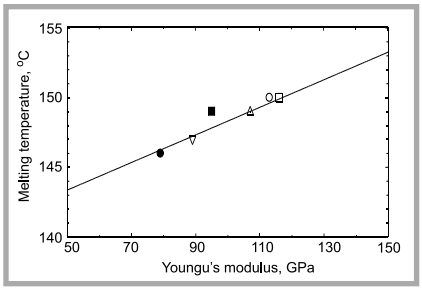

***Figure 2**. The relationship between the tensile modulus and the melting temperature (Tm) of gel-spun polyethylene fibres: ●, Spectra® 900; O, Spectra® 1000; □, Spectra® 2000; ∇, Dyneema® SK60, ■, Dyneema® SK65; Δ, Dyneema® SK75.*

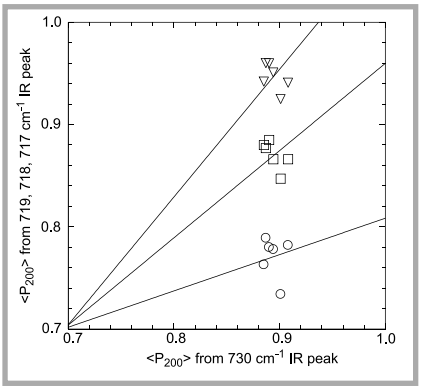

***Figure 4.** Comparison of <P_{200}> values obtained from the 730 cm-1 IR peak with those obtained from 719 (O), 718 (□) and 717 (∇) cm-1 infrared peaks.*

An analysis of the corrected half-height widths of the equatorial peak with an average d-spacing of 0.415±0.005 nm, shows the so-called crystallite sizes perpendicular to the (100) diffracting planes varying between 11 nm and 14.34 nm for the Spectra® grade PE samples, and between 11.9 nm and 19.48 nm for the Dyneema® grade PE samples. These crystallite sizes correspond up to 35 chains for the Spectra® grades, and up to 47 chains for the Dyneema® grade PE samples in the direction perpendicular to the (100) diffracting planes. The USA-made PE fibres contain up to 1225 laterally packed chains forming hexagonal structure, against up to 2209 laterally packed chains forming hexagonal structure for the European-made PE fibres. It is obvious that the increasing crystallinity and lateral perfection appear to reduce the proportion of hexagonally-packed structures.

Table 4 shows the comparison of the crystallite sizes evaluated using the corrected half-height width and the integral breadth for the (110) and (200) reflections. The integral breadth may be defined as the ratio of the peak area to the full peak height. The results suggest that the integral breadth values are always higher than the corrected half-height widths, and that the corresponding calculated crystallite sizes perpendicular to the diffracting planes from the integral breath are always lower than the crystallite sizes evaluated from the corrected half-height widths. Due to the reliability of Stoke's deconvolution procedure, which takes the full peak profile into account, it is found to be more reliable.

Polarised infrared spectroscopy data

Due to the complications arising from highly absorbent bands in the 3000-2800 cm^{-1} and 1550-1350 cm^{-1} regions, the analysis has been limited to the doublet in the 775-675 cm^{-1} region. During the curve fitting procedures, it was found necessary to resolve the peak at 718 cm^{-1} into two peaks, with positions of 719 cm^{-1} and 717 cm^{-1}, to improve the fitting. The peak at 718 cm^{-1} has been quoted in the literature [27] as arising from a combination of crystalline and non-crystalline (amorphous) phases.

730 cm^{-1} peak: According to the previous investigation [20], the bandwidth of this peak is found to vary between 5 cm^{-1} and 6.5 cm^{-1} in the spectral region studied. It has been assigned to in-phase CH_2 rocking modes for the two chains in the orthorhombic unit [27,28]. The average chain angle, <$\theta_{c,f}$>, for this peak is found to vary between 14.3 and 16.1° . The corresponding values of <P_{200}> are shown in Figure 3.

718 cm^{-1} peak: This peak is known [25] to consist of components caused by the crystalline and non-crystalline phases. The crystalline component located at 717 cm^{-1} is known to come from out-of-phase CH_2 rocking modes for the two chains in the unit cell. According to the published literature [27-29], the crystalline component of this peak arises from its monoclinic structure. The non-crystalline component located at 719 cm^{-1} is assigned to CH_2 rocking modes of chain segments in the trans conformation [24,25].

The corresponding values of <P_{200}> for the IR peak at 718 cm^{-1} resolved as a single peak are shown in Figure 3. Due to the contributions from the crystalline and non-crystalline phases, the orientation parameters obtained from this peak can be regarded as the overall orientation of the crystalline and non-crystalline phases. The <P_{200}> values from this peak are found to be slightly less than those evaluated from the refractive index data. The average chain angle, <$\theta_{c,f}$>, for this peak is found to vary between 16.1° and 18.6°.

717 cm^{-1} peak: This peak has been assigned to the out-of-phase CH_2 rocking modes in the monoclinic structure. The corresponding values for <P_{200}> for this peak are shown in Figure 4. This peak has the highest orientation parameters compared with the orientation parameters obtained from the 730 cm^{-1} peak. The average chain angle, <$\theta_{c,f}$>, for this peak is found to vary between 9.3° and 12.8°. It shows that the monoclinic structure is slightly better oriented than the orthorhombic structure.

719 cm^{-1} peak: According to the previous investigation [20], this peak is found to vary between 5 and 7.3 cm^{-1} respec-

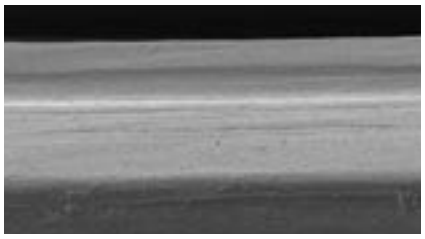

Figure 5. *Longitudinal view of Spectra® 2000 fibre (×3000).*

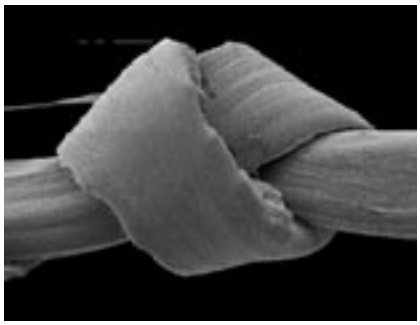

Figure 6. *Longitudinal view of Spectra® 2000 fibre with a knot (×1200).*

tively. This peak is the non-crystalline component of the peak located at 718 cm^{-1} and has been assigned to CH_2 rocking modes of chain segments in the trans conformation. According to Snyder [29], this peak is associated with sequences of more than four trans bonds, and is regarded as arising from a highly oriented hexagonal mesophase. The transition moment of this peak is also perpendicular to the chain axis, and shows perpendicular polarisation characteristics.

The corresponding values of $<P_{200}>$ are shown in Figure 3. The average chain angle for this peak, $<\theta_{c,f}>$, is found to vary between 22° and 24.9°. As shown in Figure 3, the orientation parameter of this peak, due to the non-crystalline nature of the hexagonal mesophase, is as expected lower than the orthorhombic and monoclinic structures.

Scanning electron microscopy (SEM) observations

The lateral and cross-sectional surface structures of gel-spun polyethylene fibres were examined using an ISI-100A Scanning Electron Microscope with a voltage setting of 5 kV, and a specimen to detector distances ranging between 8 mm to 12 mm respectively. As shown in Figure 5, the longitudinal SEM images are characterised by fibrillar structures running along the fibre axis direction. As the tensile modulus is increased, the surface morphology of the fibres appear to become smoother. Lower-modulus sample surfaces appear to be rougher, with fibrillar formations running in deep grooves along the fibre axis direction. The depth of the grooves become shallower as the sample surfaces become smoother. Due to the difficulties with preparing the cross-sectional samples, no high-quality images were obtained. However, the cross-sectional images appear to vary from deformed triangular shapes to deformed circular shapes, possibly due to the effects of solution spinning followed by drawing at very high draw ratios, causing the cross-sectional shapes to deform considerably. Unlike the aramids, gel-spun PE fibres showed no fibrillation or delamination when the fibre was knotted (Figure 6). The good bending behaviour is an advantage for the fabric formation. During the weaving and knitting operations, the fabric is expected to form with relative ease.

Conclusions

The structure-property relationships of commercially available high-strength, high-modulus PE fibres have been investigated utilising a combination of techniques involving optical microscopy, thermal and X-ray diffraction analysis, together with polarised IR spectroscopy techniques. Close examination of wide-angle X-ray diffraction, polarised IR spectroscopy and thermal analysis confirms the presence of three-phase structure.

The results from the birefringence measurements via the refractive index data and the polarised IR data show that the gel-spun polyethylene fibres consist of highly aligned chains along the fibre axis direction. The results show that the orientation parameter $<P_{200}>$, obtained from the dichroic ratios of 730, 719 and 717 cm^{-1} IR peaks assigned to the orthorhombic, oriented non-crystalline and monoclinic phases, shows that the monoclinic crystallites are more highly oriented than the orthorhombic crystallites. In turn, the orientation parameters of orthorhombic and monoclinic crystallites are found to be higher than that of the oriented non-crystalline structure.

Careful analysis of the wide-angle X-ray diffraction data, following the curve fitting and instrumental broadening correction procedures, shows that the USA-made Spectra® grade PE fibres contain larger laterally packed orthorhombic structures than the European-made Dyneema® grade PE fibres, as shown by the higher number of chains in the direction perpendicular to the (110) diffracting planes.

Analysis of the equatorial peak with an average d-spacing of 0.415±0.005 nm, assigned to the (100) reflection of the hexagonal structure, shows that the USA-made PE fibres contain up to 1225 laterally packed chains forming hexagonal structure, against up to 2209 laterally packed chains forming hexagonal structure for the European-made PE fibres. It is obvious that increasing crystallinity and lateral perfection appears to be reducing the proportion of hexagonally-packed structures.

As shown in Figure 2, there is a direct relationship between the tensile modulus and the melting temperature. There is also a similar relationship between the tensile modulus and/or tensile strength and the melting enthalpy, DSC crystallinity, birefringence and Herman's orientation parameter ($<P_{200}>$) values obtained from 730, 718 and 717 cm^{-1} IR peaks. Unfortunately, owing to the unavailability of processing parameters for commercial reasons, no relationship between the structure, property, and processing parameters can be established

Close examination of SEM showed that the lateral surface structures of the samples are characterised by fibrillar formations running along the fibre axis direction. Lower-modulus samples appear to have rougher surfaces becoming smoother with increasing modulus. Excellent bending behaviour was observed with the knotted single filaments, making the formation of the fabric a simple task.

The use of transmission electron microscopy (TEM) would be useful for directly measuring the crystallite size as a means of assessing the apparent crystallite sizes evaluated by the X-ray diffraction technique.

Using the high-temperature X-ray diffraction technique would provide valuable information on crystallinity, crystallite size and the orientation parameters of crystalline structures, as a function of temperature, during the phase transitions. With high-temperature IR microscopy, orientation parameters for crystalline

and non-crystalline phases, as well as further clarification of the assignments of IR peaks as a function of temperature, could be obtained, especially during the pre-melting, melting and post-melting temperatures.

Acknowledgments

- *This article is dedicated to Prof. A.K. Bilisik on the occasion of his 46th birthday.*
- *The author would like to thank DSM of Holland and Allied Signal Inc. (now Honeywell International Inc) for supplying the samples investigated in the present study. Thanks also go to Volkan Unsal and Alison Edmed for assistance with the data collection. The help and assistance of Trevor Jones of the Department of Textiles of UMIST (UK) is very much appreciated with the SEM images.*

References

1. *P.J. Brown, I. Karacan, J. Liu, J.E. McIntyre, A.H. Milburn and J.G. Tomka; Polym. Int., 1991, Vol. 24, pp 23-32*
2. *D.J. Johnson, I. Karacan, P.E.P. Maj, and J.G. Tomka; Polymer, 1990, Vol. 31, pp 1991-1998*
3. *A.B. Erdemir, D.J. Johnson, I. Karacan, and J.G. Tomka; Polymer, 1988, Vol. 29, pp 597-604*
4. *D.J. Johnson, I. Karacan, and J.G. Tomka; Polymer, 1990, Vol. 31 pp 8-14.*
5. *D.J. Johnson, I. Karacan and J.G. Tomka; Polymer, 1991, Vol. 32, pp 2312-2318.*
6. *D.J. Johnson, I. Karacan and J.G. Tomka; Polymer, 1992, Vol. 33, pp 983-989.*
7. *G. Capaccio and I.M. Ward; Nature (Phys.Sc.), 1973, Vol. 243, pp 143-143.*
8. *G. Capaccio and I.M. Ward; Polymer, 1975, Vol. 16, pp 239-243.*
9. *J.H. Southern and R.S. Porter; J. Appl. Poly. Sci., 1970, Vol. 14, pp 2305-2317.*
10. *P. Smith and P.J. Lemstra; J. Mat. Sci.; 1980, Vol. 15, pp 505-514.*
11. *P.J. Lemstra and R. Kirschbaum, Polymer, 1985, Vol. 26, 1372-1384.*
12. *http://www.spectrafibre.com; http:// www.dsm.com*
13. *D. Green, and D.I. Bower; Spectrochemica Acta.: Part A, No.8, 1993, Vol. 49A, pp 1191-1194.*
14. *I. Karacan, A Taraiya, D.I. Bower, and I.M. Ward; Polymer, 1993, Vol. 34, pp 2691-2701.*
15. *I. Karacan, D.I. Bower, and I.M. Ward; Polymer, 1994, Vol. 35, pp 3411-3422.*
16. *F. Bozdogan and I. Karacan J. Mat. Sci. Tech. 2000, Vol. 8, No. 3, pp 119-139.*
17. *A.M. Hindeleh, D.J. Johnson, and P.E. Montague; 'Fibre Diffraction Methods', ACS Symp. No. 141 (Eds. A.D. French and K.H. Gardner), American Chemical Society, Washington DC, 1983, pp 149-182.*
18. *A.R. Stokes; Proc. Phys. Soc., 1948, Vol. A61, pp 382-391.*
19. *H. de Vries; Colloid & Polym.Sci., 1979, Vol: 257, pp226 238.*
20. *B. Wunderlich; Macromolecular Physics 1980, Vol: 3, 69.*
21. *W. Hu, A. Buzin, J. S. Lin, and B. Wunderlich; J. Poly. Sci.: Part B: Poly.Phys., 2003, Vol: 41, pp 403 - 417.*
22. *J. Pak, and B. Wunderlich; Thermochimica Acta, 2004, Vol. 421, pp. 203 - 209.*
23. *Y. K. Kwon, A. Boller, M. Pyda, and B. Wunderlich; Polymer, 2000, Vol: 41, pp. 6237 - 6249.*
24. *S. Krimm; Fortschr. Hochpolym. –Forsch, 1960, Vol. 2, pp. 51 - 172.*
25. *B. E. Read and R. S. Stein; Macromolecules, 1968, Vol. 1, No. 2, pp. 116-126.*
26. *R. G. Snyder, J. Chem. Phys., 1979, Vol: 71(8), pp. 3229-3235.*
27. *A. Kaito, K. Nakayama, and H. Kanetsuna, J. Macromol.Sci. 1987, Vol. B26(3), 281*
28. *R. K. Krishnaswamy; J. Polym. Sci., Part B: Polym.Phys. 2000, Vol: 38, 182.*
29. *K. M. Furuheim, D. E. Axelson, H. W. Antonsen, and T. Helle; J. Appl. Poly. Sci. 2004, Vol. 91, 218.*

Received 10.01.2005 Reviewed 24.06.2005